

Quantum Monte Carlo Calculations for Solids Using Special k Points Methods

G. Rajagopal,¹ R. J. Needs,¹ S. Kenny,¹ W. M. C. Foulkes,² and A. James²

¹*Cavendish Laboratory, Madingley Road, Cambridge CB3 0HE, United Kingdom*

²*The Blackett Laboratory, Imperial College, Prince Consort Road, London SW7 2BZ, United Kingdom*

(Received 4 March 1994)

We describe a quantum Monte Carlo method for calculating the electronic properties of solids using wave functions with nonzero wave vectors. Our method uses the idea of “special k points” derived from band structure theory, and leads to greatly improved accuracy for insulating systems. We illustrate our method with calculations on germanium in the diamond structure.

PACS numbers: 71.10.+x, 71.20.Ad

Variational and diffusion quantum Monte Carlo (VMC and DMC) methods have been used in a number of studies of electronic systems, such as atoms and molecules [1], the homogeneous electron gas (jellium) [2], a jellium surface [3], phases of solid hydrogen [4], and solids composed of heavier atoms such as carbon [5] and silicon [5,6]. The accuracy of a VMC calculation is ultimately limited by the quality of the many-body wave function used. DMC calculations can, in principle, give exact energies, but in practice the so-called fixed-node approximation [1,2] is normally used for large systems, in which the nodal surface of the wave function is constrained to be equal to that of an approximate wave function. In many applications the fixed-node approximation has given excellent results, and the DMC technique is one of the most promising methods for accurate calculations on many-body electronic systems.

Calculations for solids have used a supercell method with a many-body wave function satisfying periodic boundary conditions, which reduces the problem to one involving a finite number of electron coordinates [2–6]. An extrapolation to infinite-supercell size is normally required, which often involves using results from approximate methods, such as local-density-approximation (LDA) calculations [3–6], which reduces the reliability of the final results. In this paper we show that VMC and DMC methods can be used in conjunction with many-body wave functions which obey different boundary conditions from the strictly periodic ones used in previous calculations. Our method uses the ideas of “special” k points [7–9], which have been widely used in band structure calculations for insulating systems. For a given supercell size our method gives energies and electronic charge densities which are much closer to those of the ground state of the truly infinite system than previous VMC and DMC calculations. This development will allow VMC and DMC methods to be used with greater accuracy in calculating the properties of complex solids.

The Hamiltonian employed in supercell many-body calculations is of the form

$$H = -\frac{1}{2} \sum_{i=1}^N \nabla_i^2 + \sum_R \sum_{i>j}^N \frac{1}{|r_i - r_j - R|} + \sum_{i=1}^N V(r_i), \quad (1)$$

where $\{\mathbf{R}\}$ is the set of translation vectors of the supercell lattice, $V(\mathbf{r})$ has the periodicity of $\{\mathbf{R}\}$, and N is the number of electrons in the supercell. Both the Hamiltonian H and the Hamiltonian of the truly infinite system are invariant under the simultaneous translation of *all* electron coordinates by a translation vector of the crystal lattice. However, H has the additional symmetry that it is invariant under the translation of *any* electron coordinate by a vector in $\{\mathbf{R}\}$. A proof [10] following similar lines to the standard derivation of Bloch’s theorem shows that the translational symmetry of H implies that its eigenstates can be chosen to be of the form

$$\Phi_{\mathbf{k}}(\{r_i\}) = U_{\mathbf{k}}(\{r_i\}) \exp\left(ik \sum_{i=1}^N r_i\right). \quad (2)$$

In this expression \mathbf{k} is a wave vector which can be chosen to lie within the first Brillouin zone (BZ) of the supercell lattice, and $U_{\mathbf{k}}$ is invariant under translation of *any* electron coordinate by a vector in $\{\mathbf{R}\}$ [11]. In general $U_{\mathbf{k}}$ is complex, unless $\mathbf{k} = 0$, in which case $U_{\mathbf{k}}$ can be chosen to be real. Previous VMC and DMC calculations for solids have used $\mathbf{k} = 0$ wave functions; however, we will show that it is possible to use wave functions with nonzero \mathbf{k} vectors, and that this freedom can be used to improve the accuracy of the calculations considerably. The ground state for the infinite-sized supercell has $\mathbf{k} = 0$, but this is not the case for a finite-sized supercell, and we have constructed an explicit example with $N = 6$ noninteracting electrons in a fixed periodic potential where the ground state has $\mathbf{k} \neq 0$ [10]. One could perform calculations at different wave vectors for a number of purposes, but here our intention is to choose wave vectors for which the lowest energy state gives a good representation of the ground state of the infinite-sized-supercell system.

Typically the approximate wave function used in VMC calculations and the guiding wave function used in DMC calculations for solids is chosen to be of the Slater-Jastrow-Bijl form,

$$\Phi_{\mathbf{k}} = \exp\left[-\sum_R \sum_{i>j}^N u(|r_i - r_j - R|) + \sum_{i=1}^N \chi(r_i)\right] D, \quad (3)$$

where the function $u(r)$ correlates the electrons in pairs, $\chi(\mathbf{r})$ is a one-body function, and D is a determinant of single-particle states. $\chi(\mathbf{r})$ is chosen to have the periodicity of $\{\mathbf{R}\}$ (and any other symmetries of the crystal) and the u term is invariant under any translation in $\{\mathbf{R}\}$. Appropriate choices for u and χ have been discussed elsewhere [2–6], and in this paper we will mainly be concerned with the choice of the single-particle states from which the determinant D is constructed.

In order to study the properties of single-determinant wave functions it is instructive to consider solutions of the Schrödinger equation for the Hamiltonian H within a self-consistent-field approach using the LDA for the exchange-correlation energy. We have performed LDA calculations for Ge in the diamond structure with the experimental value of the cubic lattice constant of 5.65 Å. To represent the Ge^{4+} ions we used a local pseudopotential of Starkloff-Joannopoulos form [12]. The wave functions and potentials were expanded in a plane-wave basis set containing all waves up to a kinetic energy cutoff of 40 Ry. We considered 8 different sizes of supercell, the smallest of which was the primitive cell containing 2 atoms, which we refer to as a $1 \times 1 \times 1$ cell, and the largest of which was obtained by multiplying the primitive vectors by a factor of 8 to give a $8 \times 8 \times 8$ cell containing 1024 atoms. Within the LDA the wave function $\Phi_{\mathbf{k}}$ is a determinant of single-particle states, each of which has the same wave vector \mathbf{k} , when reduced into the BZ of the supercell lattice. In Fig. 1 we plot the LDA energies for the 8 supercell sizes for 3 different choices of wave vector \mathbf{k} : $\mathbf{k} = 0$, $\mathbf{k} = \mathbf{G}_{111}/2 = (\mathbf{b}_1 + \mathbf{b}_2 + \mathbf{b}_3)/2$, where the \mathbf{b}_i are the primitive-reciprocal-lattice vectors of the supercell, and $\mathbf{k} = \mathbf{k}_B$, where \mathbf{k}_B is the Baldereschi mean-value point [7] of the supercell BZ. From Fig. 1 we see that for the $\mathbf{k} = 0$ sampling the energy converges rather slowly with increasing supercell size, in contrast to the $\mathbf{k} = \mathbf{G}_{111}/2$ sampling where the convergence is much better, while the $\mathbf{k} = \mathbf{k}_B$ sampling is slightly better again. Inspection of the Fourier components of the charge density shows convergence following that of the energy, as do the kinetic, electron-ion, Hartree, and exchange-correlation terms. We conclude that, especially for small supercells, a wave function with $\mathbf{k} = \mathbf{G}_{111}/2$ or $\mathbf{k} = \mathbf{k}_B$ gives a considerably better approximation to the ground-state properties of the infinite-supercell Ge system than a $\mathbf{k} = 0$ wave function. This conclusion is entirely in accord with many previous self-consistent-field studies. Special \mathbf{k} -points techniques give excellent results when used in self-consistent-field studies of insulating systems, while for metals the improvement over $\mathbf{k} = 0$ sampling is much smaller because of the presence of partially filled bands. We expect the same considerations to apply to the use of special \mathbf{k} -points techniques in VMC and DMC calculations.

For computational efficiency when performing the LDA calculations we map the states in the supercell BZ into that of the primitive cell. The resulting mesh of \mathbf{k}

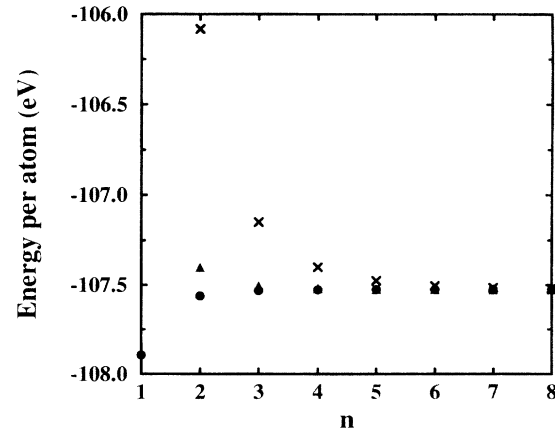


FIG. 1. LDA energies in eV per atom for $n \times n \times n$ supercells of diamond structure germanium. $\mathbf{k} = 0$ sampling (crosses), $\mathbf{k} = \mathbf{G}_{111}/2 = (\mathbf{b}_1 + \mathbf{b}_2 + \mathbf{b}_3)/2$ sampling (triangles), where the \mathbf{b}_i are the primitive-reciprocal-lattice vectors of the supercell, and $\mathbf{k} = \mathbf{k}_B$ sampling (circles) where \mathbf{k}_B is the Baldereschi mean-value point of the supercell Brillouin zone.

points is of the same type as the sets of “special” \mathbf{k} points introduced by Monkhorst and Pack [8], although we consider a mesh with an arbitrary offset from the origin [9]. In fact the $\mathbf{k} = \mathbf{G}_{111}/2$ meshes that we use for supercells which are even multiples of the primitive cell ($n \times n \times n$ cells with n even) are identical to the corresponding $n \times n \times n$ Monkhorst-Pack meshes, while for odd multiples the offset from the origin leads to a sampling which is superior to the corresponding Monkhorst-Pack mesh. The $\mathbf{k} = \mathbf{k}_B$ sampling of the $n \times n \times n$ supercell BZ gives a $n \times n \times n$ mesh of \mathbf{k} points in the primitive BZ of Monkhorst-Pack type, but offset from the origin by \mathbf{k}_B . This multipoint Baldereschi-type special \mathbf{k} points scheme, which allows accurate BZ integrations to be performed with very small numbers of \mathbf{k} points, does not appear to have been used before, and may be of use in self-consistent-field calculations, although it generates sets of \mathbf{k} points with low symmetry.

We now turn our attention to VMC calculations. Wave functions of the form of Eq. (2) can be used straightforwardly in VMC calculations. The VMC expression for the energy, E_{VMC} , is

$$E_{\text{VMC}} = \frac{\int (\Phi_{\mathbf{k}}^* \Phi_{\mathbf{k}}) (\Phi_{\mathbf{k}}^{-1} H \Phi_{\mathbf{k}})}{\int (\Phi_{\mathbf{k}}^* \Phi_{\mathbf{k}})}, \quad (4)$$

where $\Phi_{\mathbf{k}}^* \Phi_{\mathbf{k}}$ is a probability distribution, which is real and positive, and $\Phi_{\mathbf{k}}^{-1} H \Phi_{\mathbf{k}}$ is known as the local energy. In a VMC calculation the probability distribution is generated pointwise using a random walk procedure, and the local energy is accumulated (after an equilibration step) along the walk. For an arbitrary \mathbf{k} vector the local energy is complex at a general point along the walk, but in the limit of exact sampling the imaginary parts cancel from Eq. (4). If an electron coordinate is translated by a vector \mathbf{R} in the set $\{\mathbf{R}\}$ then the wave function $\Phi_{\mathbf{k}}$ is

multiplied by a phase factor $\exp(i\mathbf{k} \cdot \mathbf{R})$, which leaves both the probability distribution and the local energy unaltered. It follows that the integrals in Eq. (4) need be performed only over a single supercell in configuration space, as is the case for $\mathbf{k} = 0$ calculations. The only additional complication which arises from using wave functions of the form of Eq. (2) in a VMC calculation (with an arbitrary nonzero \mathbf{k} vector) is that in general one must use complex arithmetic to evaluate the periodic part of the wave function, $U_{\mathbf{k}}$, which costs a factor of 4 more in computing time than evaluating a real $U_{\mathbf{k}}$.

A particularly advantageous choice is $\mathbf{k} = \mathbf{G}/2$, where \mathbf{G} is any supercell-reciprocal-lattice vector. We have already seen that choosing $\mathbf{k} = \mathbf{G}_{111}/2$ for Ge gives excellent results within the LDA, even for small supercells, but another important advantage of using $\mathbf{k} = \mathbf{G}/2$ is that one can choose a wave function of the form of Eqs. (2) and (3) with a single, real determinant. The mesh generated by $\mathbf{k} = \mathbf{G}/2$, and all points which differ from it by a supercell-reciprocal-lattice vector, is invariant under inversion through the origin, and for a closed shell configuration, it is therefore possible to form linear combinations of the single-particle states which are real, which can be used to form a real determinant. We have tested this scheme by performing VMC calculations on the $2 \times 2 \times 2$ and $3 \times 3 \times 3$ Ge supercells for $\mathbf{k} = 0$ and $\mathbf{k} = \mathbf{G}_{111}/2$ wave functions. For the two-body correlation function $u(r)$ we used a standard form which is discussed, for instance, in Refs. [2] and [5], and which yields the exact behavior when two electrons approach one another, and gives the long-ranged behavior appropriate for a uniform system of the same average density. The single-particle states were calculated within the LDA and the one-body function $\chi(\mathbf{r})$ was constructed using the procedure of Ref. [5], which gives a charge density close to the LDA form. To obtain accurate statistics the averages were computed over 30 000 configurations for both the $2 \times 2 \times 2$ and $3 \times 3 \times 3$ systems.

The VMC energies are given in Table I, together with the corresponding LDA results and the LDA finite-size corrections, which are the differences between the LDA result for a particular supercell size and wave vector, and the LDA result for a very large supercell and a 40 Ry cutoff energy of -107.526 eV per atom (which is independent of the wave vector; see Fig. 1). For both supercell sizes the LDA finite-size correction using the $\mathbf{k} = \mathbf{G}_{111}/2$ wave functions is an order of magnitude smaller than the correction for $\mathbf{k} = 0$.

We now consider the case of DMC calculations. The DMC expression for the energy is

$$E_{\text{DMC}} = \frac{\int (\Psi_{\mathbf{k}}^* \Phi_{\mathbf{k}}) (\Phi_{\mathbf{k}}^{-1} H \Phi_{\mathbf{k}})}{\int (\Psi_{\mathbf{k}}^* \Phi_{\mathbf{k}})}, \quad (5)$$

where $\Phi_{\mathbf{k}}$ is the guiding wave function and $\Psi_{\mathbf{k}}$ is the best wave function consistent with the nodal surface of $\Phi_{\mathbf{k}}$. E_{DMC} is real but, for an arbitrary \mathbf{k} , the distribution $\Psi_{\mathbf{k}}^* \Phi_{\mathbf{k}}$ is complex and cannot be generated by the standard

DMC algorithm. We have not attempted to generate this distribution by a modified algorithm, but instead we have used the standard DMC algorithm with the (real) $\mathbf{k} = 0$ and $\mathbf{k} = \mathbf{G}_{111}/2$ wave functions from the VMC calculations as guiding functions, so that the distribution $\Psi_{\mathbf{k}}^* \Phi_{\mathbf{k}}$ is real and positive. The “tiling property” of ground-state fermionic wave functions [13] guarantees that all nodal cells of the wave function are equivalent and therefore a DMC calculation may be performed within a single nodal cell. It is straightforward to show that the tiling property holds under the joint action of the permutation and translational symmetry for the lowest-energy wave function at each wave vector $\mathbf{k} = \mathbf{G}/2$ [10]. Finally, as for the VMC calculations described earlier, all of the supercells in configuration space give equal contributions to Eq. (5), and the integrals need be performed only over a single supercell.

We have performed DMC calculations in the fixed-node and short-time approximations for the same $2 \times 2 \times 2$ and $3 \times 3 \times 3$ Ge supercells as used in our VMC calculations. We used a time step of 0.015 a.u., which is the same value as used in the study of Si by Li, Ceperley, and Martin [6], who demonstrated that the resultant time-step error was small in that case. The average number of configurations in the ensemble was 200, and for each configuration 3000 moves of all the electrons were attempted for the $2 \times 2 \times 2$ calculations and 500 moves for the $3 \times 3 \times 3$ calculations. The fixed-node approximation [1,2] was implemented by rejecting any moves in which a node crossing was attempted [14]. The results of the DMC calculations are given in Table I.

The calculated VMC and DMC energies may be corrected for finite-size effects by adding the appropriate LDA corrections, Δ_{LDA} , given in Table I. This procedure yields energies which are very similar for the different \mathbf{k} samplings; however, the energies for the $2 \times 2 \times 2$ supercells are 0.3–0.4 eV per atom lower than the $3 \times 3 \times 3$ results. From this we deduce that (a) the LDA-finite-size corrections work reasonably well for Ge in correcting for the different \mathbf{k} sampling at fixed supercell size, and (b) there is an additional size-dependent correction which is not included in the LDA. Conclusion (a) is to be expected for Ge, where the LDA works well; however, the most important applications of quantum Monte Carlo techniques will be to systems in which the LDA is inadequate, and in these cases we do not have a reliable scheme for calculating finite-size corrections, so that our special \mathbf{k} points method will be extremely valuable. VMC calculations for jellium [15] indicate that the additional size-dependent correction beyond the LDA is positive for system sizes and electron densities comparable to our Ge calculations, and that for a system comparable to our $3 \times 3 \times 3$ calculations this correction is small ($\sim +0.1$ eV per atom). When comparing with the LDA results we must consider the effects of basis set incompleteness in the LDA calculations. The LDA energies in Table I were calculated using a 40 Ry basis set energy

TABLE I. Energies of diamond structure germanium in eV per atom for the $2 \times 2 \times 2$ and $3 \times 3 \times 3$ supercells, using $\mathbf{k} = 0$ and $\mathbf{k} = \mathbf{G}_{111}/2$ wave functions, and the LDA, VMC, and DMC methods. Estimated statistical errors in the last decimal digit are given in brackets. Finite-size corrections, Δ_{LDA} , calculated within the LDA, are also given.

	$n \times n \times n$	E_{LDA}	E_{VMC}	E_{DMC}	Δ_{LDA}
$\mathbf{k} = 0$	$2 \times 2 \times 2$	-106.08	-106.05(2)	-106.65(7)	-1.44
	$3 \times 3 \times 3$	-107.15	-106.81(5)	-107.44(5)	-0.38
$\mathbf{k} = \mathbf{G}_{111}/2$	$2 \times 2 \times 2$	-107.40	-107.49(2)	-108.03(7)	-0.12
	$3 \times 3 \times 3$	-107.51	-107.28(2)	-107.74(4)	-0.02

cutoff. We have performed LDA calculations with various cutoffs up to 125 Ry, from which we deduce that the infinite-basis-set LDA energies are approximately 0.12 eV per atom lower than those quoted in Table I. The VMC energies are expected to be lowered by a similar amount, but the DMC results are expected to be insensitive to the basis set used for the guiding wave function, as shown in [6]. Our value for the fully converged LDA energy of -107.65 eV per atom is very close to the finite-size-corrected DMC result of -107.76 eV per atom, and because of the various uncertainties the difference between these values is not significant.

A DMC calculation for the Ge atom gave an energy of -103.42(3) eV, which is considerably lower than the (spherically symmetric and spin-polarized) LDA result of -102.80 eV. The DMC cohesive energy of 4.34 eV per atom is subject to corrections of -0.29 eV (difference between the LDA cohesive energy using a norm-conserving pseudopotential [16] and the local pseudopotential used here) and -0.04 eV (zero-point motion). The final cohesive energy of 4.01 eV is in reasonable agreement with the experimental value of 3.85 eV [17], and is much better than the LDA result of 4.59 eV [16].

In conclusion, we have described a method for performing VMC and DMC calculations for periodic solids using wave functions with nonzero wave vectors. For insulating systems and small supercells our method gives results much closer to infinite-sized-supercell results than zero-wave-vector calculations. This conclusion is in accordance with the ideas of "special \mathbf{k} points" methods which have been developed in band structure theory. A particularly advantageous choice is $\mathbf{k} = \mathbf{G}/2$, where \mathbf{G} is a supercell-reciprocal-lattice vector, which, for a closed shell configuration, allows the use of a real wave function. We have tested our method by performing calculations on Ge in the diamond structure. Our method will also be useful in studies of lattice models such as the Hubbard Hamiltonian. The freedom to use nonzero wave vectors in VMC and DMC calculations for solids can be used to achieve much more accurate results than obtained in previous work.

We thank M.Y. Chou, S. Fahy, B. Farid, and R. Haydock for helpful conversations, and the Science and Engineering Research Council (U.K.) for financial support. The computations were performed on the Cray

YMP-8 at the Rutherford-Appleton Laboratories (U.K.), and the Cray C-90 at the Pittsburgh Supercomputing Center (Grant No. DMR930039P).

- [1] P.J. Reynolds, D.M. Ceperley, B.J. Alder, and W.A. Lester, *J. Chem. Phys.* **77**, 5593 (1982); D.M. Ceperley and B.J. Alder, *ibid.* **81**, 5833 (1984); R.M. Grimes, B.L. Hammond, P.J. Reynolds, and W.A. Lester, *ibid.* **85**, 4749 (1987).
- [2] D.M. Ceperley, *Phys. Rev. B* **18**, 3126 (1978); D.M. Ceperley and B.J. Alder, *Phys. Rev. Lett.* **45**, 566 (1980).
- [3] X.-P. Li, R.J. Needs, R.M. Martin, and D.M. Ceperley, *Phys. Rev. B* **45**, 6124 (1992).
- [4] D.M. Ceperley and B.J. Alder, *Phys. Rev. B* **36**, 2092 (1987); V. Natoli, R.M. Martin, and D.M. Ceperley, *Phys. Rev. Lett.* **70**, 1952 (1993).
- [5] S. Fahy, X.W. Wang, and S.G. Louie, *Phys. Rev. Lett.* **61**, 1631 (1988); *Phys. Rev. B* **42**, 3503 (1990).
- [6] X.-P. Li, D.M. Ceperley, and R.M. Martin, *Phys. Rev. B* **44**, 10929 (1991).
- [7] A. Baldereschi, *Phys. Rev. B* **7**, 5212 (1973).
- [8] H.J. Monkhorst and J.D. Pack, *Phys. Rev. B* **13**, 5188 (1976).
- [9] W.R. Fehlner and S.H. Vosko, *Can. J. Phys.* **55**, 2041 (1978); A.H. MacDonald, *Phys. Rev. B* **18**, 5897 (1978).
- [10] G. Rajagopal, R.J. Needs, S. Kenny, W.M.C. Foulkes, and A. James (to be published).
- [11] We have omitted the band index in Eq. (2), as we will be concerned only with the lowest band.
- [12] Th. Starkloff and J.D. Joannopoulos, *Phys. Rev. B* **16**, 5212 (1977).
- [13] D.M. Ceperley, *J. Stat. Phys.* **63**, 1237 (1991).
- [14] We do not restrict the electron coordinates to a single supercell. If one wished to impose such a restriction, one would shift the electron coordinates into the chosen supercell by removing supercell translation vectors, which would multiply the wave function by a phase factor and may involve moving to a new nodal cell. Such a move to a new nodal cell must *not* be regarded as an attempt to cross the nodal surface.
- [15] L. Fraser, W.M.C. Foulkes, G. Rajagopal, and R.J. Needs (to be published).
- [16] B. Farid and R.J. Needs, *Phys. Rev. B* **45**, 10647 (1992).
- [17] C. Kittel, *Introduction to Solid State Physics* (Wiley, New York, 1986), 6th ed., p. 55, Table I. These data were supplied by L. Brewer (after LBL Report No. 3720 Rev.).